

# Extended Mathematical Expression of BER for MB-UWB System in Underground Mine Channel

Athar Ravish Khan Sanjay M. Gulhane

**Abstract-** The IEEE802.15.3a cluster-based channel model has been adapted for Ultra Wideband (UWB) system. The suggested realistic channel is assessed by its distribution of fading amplitude and time of arrivals. Yanjing Sun et al. use this model as a basis to improve the channel model for underground mine. In this paper we present the closed form expression of bit-error-rate (BER) of uncoded and convolution coded Multi Band Orthogonal Frequency Division Multiplexing (MB-OFDM) UWB system in terms channel parameters of UWB channel, using Gauss-Hermite quadrature integration. This paper provides weight and zeros of Hermite polynomial, error weights of Hamming Distant for Rayleigh fading for convolution coding and simulated time and frequency domain signal of MBOFDM. Theoretical and simulation analysis of MBOFDM have been performed for IEEE UWB channel and underground mine channel model. The analytical result is validated with simulation.

**Keywords:** MBOFDM, UWB Channel, Underground mine Channel, BER.

## I. INTRODUCTION

Mining industry is one of the most difficult industries, concerning production and technological processes. Underground mines, which are characterized by their tough working conditions and hazardous environments, require foolproof mine-wide communication systems for smooth functioning of mine workings and ensuring better safety. With its enormous bandwidth, UWB provides a promising solution to satisfy these requirements. UWB communication approaches can be categorized into two main approaches: single-band and multiband. Building high-speed RF circuit and processing a very large bandwidth are difficult issues in single band UWB. Also, large number of multipath components increases the complexity of single band receiver. Underground mine channel shows harsh multipath environment. MBOFDM presents high robustness against multipath and for high data rates MBOFDM scheme outperform the single band UWB [19]. Also, compare to Multi Band UWB, single band techniques need more complex timing synchronization to achieve an acceptable performance and hence MBOFDM seems to be a promising technique for underground mine communication. In this paper the attempt is made to evaluate the MBOFDM UWB system for underground mine channel. D.Sen *et al.* [6] has presented the closed form expression of BER of a convolution coded MB-OFDM UWB system excluding clustering parameter of UWB channel. In this paper we have attempted to extend the expression derived in [6] by incorporating power decay coefficient for clusters( $\Gamma$ ), power decay coefficient for pulse with in clusters ( $\gamma_{ch}$ ), cluster average arrival rate ( $\Lambda$ ) and pulse average arrival rate( $\lambda$ ) with in clusters of IEEE UWB channel, and validate the analytical result with the simulation results.

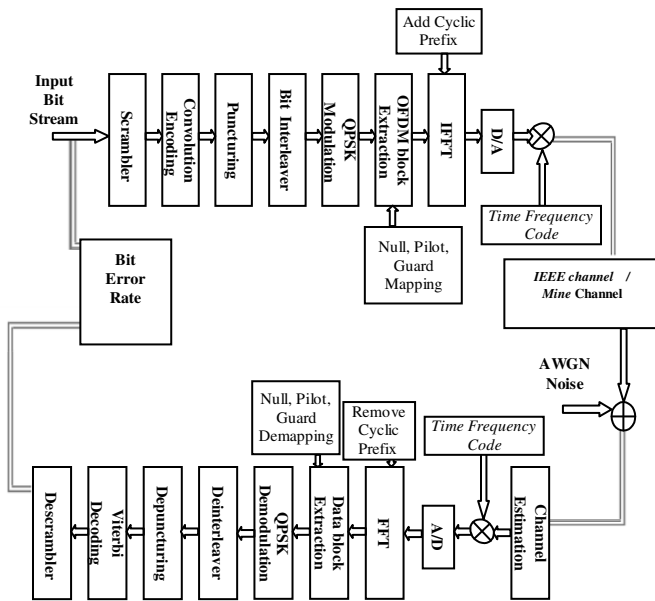
Section II presents key points of IEEE 802.15.3a WPAN standard (TG3a) proposal for MBOFDM UWB system [1]. Section III and IV presents the BER analysis for uncoded and convolution coded system respectively. Section V deals with channel model for underground mine; following the simulation results for validation of analysis in section VI. Section VII concludes the results.

## II. MULTIBAND OFDM

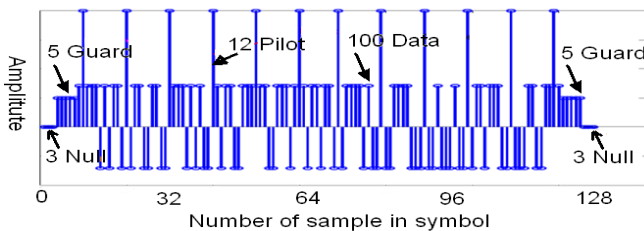
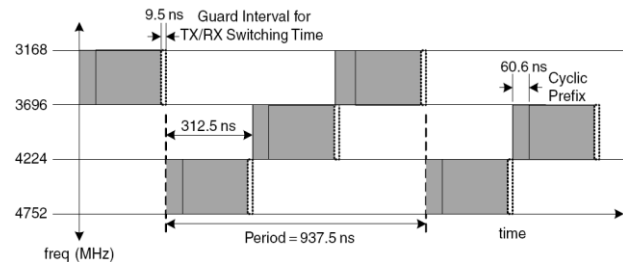
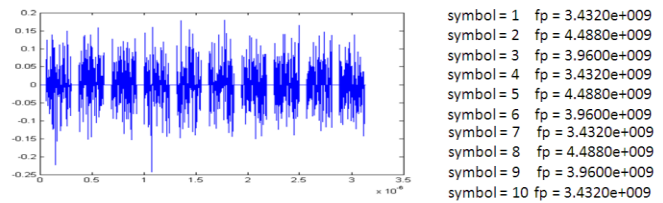
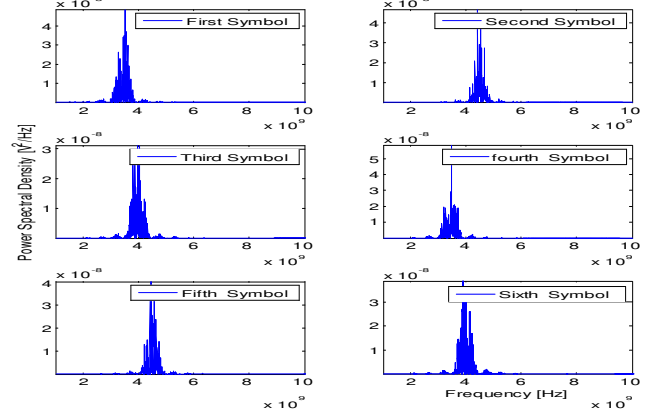
In the proposal of IEEE 802.15.3a WPAN standard (TG3a) for multiband OFDM, the UWB signal occupies 528 MHz of bandwidth, allowing 14 such signals to cover the entire 7.5-GHz band [1]. The total allocated band is divided into four band groups with three bands each, and one band group with two bands. Band group one, which include the three lowest frequency bands, is mandatory for all MBOFDM compatible devices. Each 528MHz band uses by OFDM is divided into a set of orthogonal narrow band channels. Each OFDM symbol has 128 subcarriers, and quadrature phase shift keying (QPSK) is used to modulate the transmitter signal at the subcarriers. The system provides a wireless communication with data-rates of 53.3 to 480 Mbps [2]. The block schematic of MBOFDM UWB system describe in IEEE TG3a proposal is shown in Fig.1 [2]. The first block is a data scrambler, the digital information is then encoded using convolutional encoder for error correction. Different coding rates are generated by puncturing and depuncturing. To provide robustness against burst errors, the coded bits are interleaved prior to modulation. Following the interleaving, the binary data is divided into groups of two bits and converted into complex numbers, which are representing QPSK constellation points. Data blocks each of 100 complex number are extracted to form OFDM symbol [1] to which 12 pilot, 10 guard and 6 null

**TABLE 1**  
**TIMING PARAMETER OF MBOFDM**

Parameter	Value
Number of OFDM subcarriers	128
Number of data subcarriers	100
Number of defined pilot subcarriers	12
Number of guard subcarriers	10
$\Delta f$ : Subcarrier frequency spacing	4.125 MHz
$T_{FFT}$ : IFFT/FFT period	242.42 ns ( $1/\Delta f$ )
$T_{CP}$ : Cyclic prefix duration	60.61 ns ( $=32/528$ MHz)
$T_{GI}$ : Guard interval duration	9.47 ns ( $=5/528$ MHz)
$T_{SYM}$ : Symbol duration	312.5 ns ( $T_{FFT} + T_{CP} + T_{GI}$ )


**Figure 1: MBOFDM system**

samples are added as shown in Fig. 2, to take 128 point IFFT as per timing parameters shown in Table.1. After performing the IFFT, a zero-padded suffix of length 37 is appended to the IFFT output to mitigate the effects of multipath as well as to provide a guard period to allow for switching between the different bands. The final number of samples per OFDM symbol is 165. The transmitter and receiver architectures for a MBOFDM system are very similar to that of a conventional wireless OFDM system. The main difference is that the multiband OFDM system uses a time–frequency kernel to specify the center frequency for the transmission of each OFDM symbol after digital to analog conversion of signals. An example of one realization of a time–frequency code is shown in Fig. 3. In this paper, we used MB OFDM system employing three sub-bands and a time-frequency code [1,3,2] of length 3 [2]. Time domain and frequency domain representation of MBOFDM signal is as shown in Fig. 4 and Fig. 5 respectively [3]. At the receiver perfect channel estimation is assume. Signals are demodulated using time frequency kernel and reconstructed. The guard interval and zero padding is removed and the remaining 128 samples of OFDM symbols are then recovered using Fast Fourier Transform (FFT). The tones are obtained by QPSK demodulation following deinterleaving and depuncturing, and the binary data is recovered using Viterbi decoder and descrambling.


**Figure 2: Structure of MBOFDM symbol**

**Figure 3: Realization of a time–frequency code**

**Figure 4: Time domain MBOFDM signal**

**Figure 5: Frequency domain MBOFDM signal**

### III. BER OF UNCODED MBOFDM SYSTEM

For the fading channel like UWB in WPAN, the average BER evaluated by integrating the Gaussian Q-function over fading probability density function (PDF) is given by [4]

$$P_e = \int_0^{\infty} Q(a\sqrt{\gamma}) p_{\gamma}(\gamma) d\gamma \quad (1)$$

where  $p_\gamma(\gamma)$  is PDF of instantaneous SNR per bit  $\gamma$ ,  $a$  is constant which depends on specific modulation and  $Q$  is Gaussian Q-function given by,

$$Q(x) = \int_x^\infty \frac{1}{\sqrt{2\pi}} \exp(-y^2/2) dy \quad (2)$$

The truncation of the upper infinite limit of integration and the presence of the argument of the function as the lower limit of the integral are the difficulties in classical definition of Gaussian Q-function in (2). The alternative definition of Q-function defined by [4] to solve the above difficulties is given as

$$Q(x) = \frac{1}{\pi} \int_0^\pi \exp(-x^2/2\sin^2\theta) d\theta \quad \text{for } x \geq 0 \quad (3)$$

this Q-function has finite integration limits which are not depend on the argument of function  $x$ . Using (3), the average BER leads to

$$P_e = \int_0^\pi \int_0^\infty \exp(-(a\sqrt{\gamma})^2/2\sin^2\theta) p_\gamma(\gamma) d\gamma d\theta$$

$$P_e = \frac{1}{\pi} \int_0^\pi \int_0^\infty \exp(-(a^2\gamma)/2\sin^2\theta) p_\gamma(\gamma) d\gamma d\theta \quad (4)$$

the PDF of UWB Channel can be expressed as in [4]

$$p_\gamma(\gamma) = \frac{10 \ln 10}{\sqrt{2\pi\sigma^2\gamma}} \exp \left[ \frac{-(10 \log_{10} \gamma - \mu)^2}{2\sigma^2} \right]$$

where  $\gamma \geq 0$ ,  $\mu_{dB} = \overline{10 \log_{10} \gamma}$  is logarithmic mean of  $\gamma$ ,

$\sigma_{dB}$  = Logarithmic standard deviation of  $\gamma$

Considering log-normal fading of UWB channel the average BER leads to

$$P_e = \frac{1}{\pi} \int_0^\pi \int_0^\infty \exp(-(a^2\gamma)/2\sin^2\theta) \frac{10 \ln 10}{\sqrt{2\pi\sigma^2\gamma}} \exp \left[ \frac{-(10 \log_{10} \gamma - \mu)^2}{2\sigma^2} \right] d\gamma d\theta \quad (5)$$

let  $x = \frac{-(10 \log_{10} \gamma - \mu)}{\sqrt{2\sigma}}$  then  $\gamma = 10^{(x\sqrt{2}\sigma + \mu)/10}$

$$P_e = \frac{1}{\pi} \int_0^\pi \int_{-\infty}^\infty \exp(-(a^2\gamma)/2\sin^2\theta) 10^{(x\sqrt{2}\sigma + \mu)/10} \exp(-x^2) dx d\theta \quad (6)$$

The inner integral can be efficiently computed using a Gauss-Hermite quadrature integration [5], that is

TABLE 2  
PARAMETER OF HERMITE POLYNOMIAL

i	Weight (W)	X <sub>i</sub>
1	2.229393645534e-13	-5.3874808900112
2	4.399340992273e-10	-4.6036824495507
3	1.086069370769e-07	-3.9447640401156
4	7.802556478532e-06	-3.3478545673832
5	2.283386360163e-04	-2.7888060584281
6	3.243773342238e-03	-2.2549740020893
7	2.481052088746e-02	-1.7385377121166
8	1.090172060200e-01	-1.2340762153952
9	2.866755053628e-01	-0.7374737285454
10	4.622436696006e-01	-0.2453407083009
11	4.622436696006e-01	0.2453407083009
12	2.866755053628e-01	0.7374737285454
13	1.090172060200e-01	1.2340762153953
14	2.481052088746e-02	1.7385377121166
15	3.243773342238e-03	2.2549740020893
16	2.283386360163e-04	2.7888060584281
17	7.802556478532e-06	3.3478545673832
18	1.086069370769e-07	3.9447640401156
19	4.399340992273e-10	4.6036824495507
20	2.229393645534e-13	5.3874808900112

$$\int_{-\infty}^\infty x^2 f(x) dx = \sum_{i=1}^n W_i f(x_i^{(n)}) \quad (7)$$

Where  $\{x_i\}$ ,  $i = 1, 2, \dots, n$  are the zeros of the  $n^{\text{th}}$  order Hermite polynomial and  $\{W_i\}$ ,  $i = 1, 2, \dots, n$  are corresponding weight factors tabulated in Table.2 [5] for values of order 20. The inner integral of (6) using Hermite polynomial can be written as

$$\frac{1}{\sqrt{\pi}} \int_{-\infty}^\infty \exp(-(a^2\gamma/2\sin^2\theta) 10^{(x\sqrt{2}\sigma + \mu)/10}) \exp(-x^2) dx = \frac{1}{\sqrt{\pi}} \sum_{i=1}^n W_i \exp(-(a^2\gamma/2\sin^2\theta) 10^{(x_i\sqrt{2}\sigma + \mu)/10}) \quad (8)$$

therefore average BER leads to

$$P_e = \frac{1}{\pi^{3/2}} \sum_{i=1}^n W_i \int_0^\pi \exp(-(a^2\gamma/2\sin^2\theta) 10^{(x_i\sqrt{2}\sigma + \mu)/10}) d\theta \quad (9)$$

The IEEE proposal for MBOFDM [1] recommends QPSK modulation for high and low data rates. The symbol error probability for QPSK modulation is given in [4] as

$$P(E) = \frac{1}{\pi} \int_0^\pi \exp(-E_s g_{psk} / N_o \sin^2\theta) d\theta$$

$$\text{where } g_{psk} = \sin^2\left(\frac{\pi}{M}\right)$$

and for QPSK  $M=4$  and for bit error probability  $E_s=E_b$

$$P(E) = \frac{1}{\pi} \int_0^{(M-1)\pi} \exp\left(-\frac{E_b}{N_0} \frac{1}{2\sin^2\theta}\right) d\theta \quad (10)$$

Using (9) and (10) bit error probability can be express as given in D.Sen et al. [6]

$$P_e = \frac{1}{\pi^{3/2}} \sum_{i=1}^n W_i \int_0^{3\pi/4} \exp\left[-10^{(x\sqrt{2}\sigma+\mu)/10} \frac{E_b}{N_0} \frac{1}{2\sin^2\theta}\right] d\theta \quad (11)$$

The channel impulse response of the IEEE model can be express as [7]

$$h(t) = X \sum_{n=1}^N \sum_{k=1}^{K(n)} \alpha_{nk} \delta(t - T_n - \tau_{nk}) \quad (12)$$

where  $X$  is a lognormal distributed random variable representing the magnitude of channel gain.

$$X = 10^{\frac{g}{20}}$$

where  $g$  is Gaussian random variable with mean  $g_0$  and variance  $\sigma^2$ ,  $N$  is the observed number of clusters,  $K(n)$  is the received number of multipath in the  $n^{th}$  cluster,  $\alpha_{nk}$  is coefficients of the  $k^{th}$  path in the  $n^{th}$  cluster.  $T_n$  is the arrival time of the  $n^{th}$  cluster,  $\tau_{nk}$  is the  $k^{th}$  path delay in the  $n^{th}$  cluster. The channel fading coefficient  $\alpha_{nk}$  can be define as follows [8]

$$\alpha_{nk} = p_{nk} \beta_{nk} \quad (13)$$

where  $p_{nk}$  is a discrete random variable assuming  $\pm 1$  with equal probability and  $\beta_{nk}$  is the log-normal distributed channel coefficient of  $k^{th}$  multipath belonging to  $n^{th}$  cluster. The  $\beta_{nk}$  term can thus be express as follows:

$$\beta_{nk} = 10^{\frac{x_{nk}}{20}}$$

where  $x_{nk}$  is assume to be Gaussian random variable. Variable  $x_{nk}$  in particular, can be further decomposed as follows:

$$x_{nk} = \mu_{nk} + \zeta_{nk} + \delta_{nk}$$

where  $\zeta_{nk}$  and  $\delta_{nk}$  are two Gaussian random variables that represent the fluctuations of the channel coefficient on each cluster and for pulse within each cluster, respectively. The  $\mu_{nk}$  that is the mean value of channel amplitude is determined to reproduce the exponential power decay for the amplitude of

the cluster and for the amplitude of multi-path contribution within each cluster. One can thus write.

$$\begin{aligned} \langle |\beta_{nk}|^2 \rangle &= \left\langle 10^{\frac{\mu_{nk} + \zeta_{nk} + \delta_{nk}}{20}} \right\rangle^2 = \left\langle |\beta_0|^2 \right\rangle e^{\Gamma} e^{-\frac{\tau_{nk}}{\gamma_{ch}}} \\ \Rightarrow \mu_{nk} &= \frac{10 \log_e \langle |\beta_{nk}|^2 \rangle - 10 \frac{T_n}{\Gamma} - 10 \frac{\tau_{nk}}{\gamma_{ch}}}{\log_e 10} - \frac{(\alpha_{\zeta}^2 + \alpha_{\delta}^2) \log_e 10}{20} \end{aligned} \quad (14)$$

where  $\beta_0$  represents the average energy of the first path of the first cluster, while  $\Gamma$  and  $\gamma_{ch}$  are the power decay coefficient

for clusters and pulse with in clusters respectively. The parameter in (14)  $T_n$  and  $\tau_{nk}$  depends on the cluster average arrival rate ( $\Lambda$ ) and pulse average arrival rate ( $\lambda$ ) respectively [7],[8]. With reference to (12) the fading amplitudes of UWB channel can be express as,

$$\{\alpha_{UWB}(\Gamma, \gamma_{ch}, \Lambda, \lambda)\}_{l=1}^{L_p} = \{X \alpha_{nk}\}_{l=1}^{N \times K} \quad (15)$$

where  $L_p = N \times K$ . The instantaneous SNR per bit  $\gamma_{UWB}$  of UWB channel can be expressed as

$$\gamma_{UWB}(\Gamma, \gamma_{ch}, \Lambda, \lambda) = \alpha_{UWB}(\Gamma, \gamma_{ch}, \Lambda, \lambda)^2 \frac{E_b}{N_0} \quad (16)$$

the mean  $\mu$  and standard deviation  $\sigma$  of instantaneous SNR per bit  $\gamma_{UWB}$  as a function of  $\Gamma$ ,  $\gamma_{ch}$ ,  $\Lambda$  and  $\lambda$  for UWB channel can be written as

$$\mu_{UWB}(\Gamma, \gamma_{ch}, \Lambda, \lambda) = 10 \log_{10} \overline{\gamma_{UWB}} \quad (17)$$

$$\sigma_{UWB}(\Gamma, \gamma_{ch}, \Lambda, \lambda) = \sqrt{\frac{\sum_{i=1}^{L_p} (\gamma_{UWB_{idB}}(\Gamma, \gamma_{ch}, \Lambda, \lambda) - \mu_{UWB}(\Gamma, \gamma_{ch}, \Lambda, \lambda))^2}{(L_p - 1)}} \quad (18)$$

Using (11) and (15)-(18) average BER for MBOFDM with QPSK modulation in UWB channel leads to

$$P_e(\Gamma, \gamma_{ch}, \Lambda, \lambda) = \frac{1}{\pi^{3/2}} \sum_{i=1}^n W_i \int_0^{3\pi/4} \exp\left[-10^{(x\sqrt{2}\sigma_{UWB}+\mu_{UWB})/10} \frac{E_b}{N_0} \frac{1}{2\sin^2\theta}\right] d\theta \quad (19)$$

#### IV. BER OF CODED MBOFDM SYSTEM

The bit error probability of a convolution code with code rate  $R_{cc}$  is upper bounded by

$$P_{e(coded)} < \sum_{d=d_{free}}^{\infty} C_d^- P_d^- \quad (20)$$

where,  $P_d^-$  is the pair-wise error probability with Hamming distance  $d^-$ .  $C_d^-$  is the sum of bit errors (information error weight) for events of distance  $d^-$ , and  $d_{free}$  is the free distance of the code. Assuming ideal synchronization and Viterbi decoder,  $P_d^-$  for QPSK modulated bits transmitted over UWB log normal fading channel can be written as

$$P_{d(UWB)}(\Gamma, \gamma_{ch}, \Lambda, \lambda) = \frac{1}{\pi} \int_0^{3\pi/4} \left\{ \frac{1}{\sqrt{\pi}} \sum_{i=1}^n W_i \exp\left[-10^{(x\sqrt{2}\sigma_{UWB}+\mu_{UWB})/10} R_{cc} \frac{E_b}{N_0} \frac{1}{2\sin^2\theta}\right] \right\}^{d^-} d\theta \quad (21)$$

As the weights of Hermite polynomial are independent of  $\theta$ , the above expression can be rewritten as

$$P_{\tilde{d}(UWB)}(\Gamma, \gamma_{ch}, A, \lambda) =$$

$$\frac{1}{\pi} \frac{1}{(\sqrt{\pi})^{\tilde{d}}} \sum_{i=1}^n W_i \int_0^{3\pi/4} \left\{ \exp \left[ -10^{(x_i \sqrt{2} \sigma_{UWB} + \mu_{UWB})/10} R_{cc} \frac{E_b}{N_0} \frac{1}{2 \sin^2 \theta} \right] \right\}^{\tilde{d}} d\theta$$

the upper bound of BER  $P_{e(coded)}$  for convolutional coded MBOFDM system with known channel information and perfect synchronization can be express as

$$P_{e(coded)} < \sum_{\tilde{d}=free}^{\infty} C_{\tilde{d}} P_{\tilde{d}(UWB)}(\Gamma, \gamma_{ch}, A, \lambda) \quad (22)$$

## V. UNDERGROUND MINE UWB CHANNEL MODELING

A significant number of theoretical analyses and experiments have been conducted on radio channel characteristics in underground Mines. Wang Yanfen [10] proposed a LOS UWB semi-deterministic model with double cluster statistic, which is depend on the testing environments of A.Chehri *et.al* [11],[12] and IEEE 802.15.3a indoor multipath model [8]. Reference [13], gives a coal mine multipath channel characteristics and corresponding model parameters. Yanjing Sun [14] use the IEEE802.15.3a channel model as a basis to improve the channel model for underground mine. In order to determine the values of parameters, first they obtain statistical parameters of underground mine then they use the fitting

parameter of IEEE UWB Channel and parameter of undergrounds mine channel. We simulate the channel models by using the parameter given in Table 3. From discrete time impulse response of IEEE UWB channel and underground mine channel, it can be seen that before 100ns and 300ns the amplitude fading lentamente, here the model is able to best fit the channel propagation law. Discrete time impulse response of IEEE UWB channel and underground mine channel, is as shown in Fig.6 and Fig.7 respectively [15], [16]. We compare the performance of both the channel by considering Mean Excess Delay, *RMS* (Root Mean Square) delay and number of significant paths with in 10 dB of peak (NP<sub>10dB</sub>) and observe a large increase in delays and significant paths in underground mine channel. Table 4 shows the mean value of excess delay, RMS delay and NP<sub>10dB</sub>. [16].

TABLE 3  
CHANNEL PARAMETER

Parameter	IEEE Channel	Underground Mine [14]
$\Lambda(1/ns)$	0.0233	0.0667
$\lambda(1/ns)$	2.5	2.1
$\Gamma$	7.1	36
$\gamma_{ch}$	4.3	24
$\sigma_{\xi}(dB)$	3.3941	3.3941
$\sigma_{\delta}(dB)$	3.3941	3.3941
$\sigma_{\alpha}(dB)$	3	3

TABLE 4  
SIMULATED VALUE OF CHANNEL PARAMETER

Parameter	IEEE	Mine
	Channel	Channel
Mean Excess Delay (nS)	5.0482	51.0854
Mean RMS Delay (nS)	5.4440	42.0112
Mean NP <sub>10dB</sub>	12.5100	68.0400

## 6. SIMULATION AND RESULTS

The BER is largely depends on information error weight .We have chosen the matching error weights of optical distance spectrum convolutional codes given in [9] and due to unavailability of error weights for lognormal fading channel, we have used error weights of Rayleigh fading which are given in Table 5 [6] ,[9] to plot (22). The theoretical and simulated BER performance without convolution coding in IEEE UWB channel and underground mine channel is shown

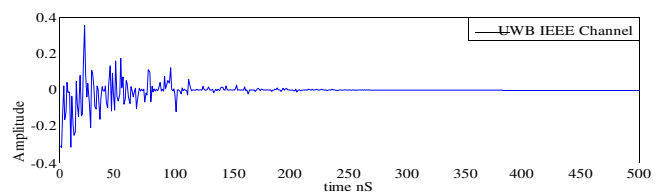


Figure 6: Discrete time impulse response of IEEE UWB channel

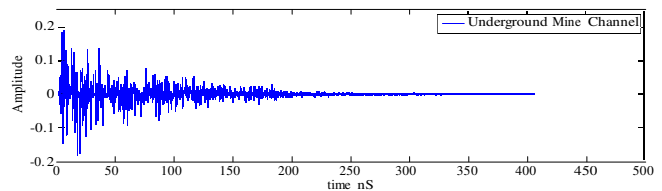


Figure 7: Discrete time impulse response of Mine Channel

in Fig. 8 and with convolution coding is shown in Fig. 9. Equation (19) is used to plot BER of uncoded system and (22) is used for coded system. Convolution code is used with constraint length  $k = 7$  and rate 1/3 is converted into rate of 1/2 using puncturing matrix  $\begin{bmatrix} 1 & 0 & 1 \end{bmatrix}$  to get the data rate of 320Mbps. OFDM symbols are transmitted over 3 frequency bands of band group 1. Simulations are carried out for 2000 noisy realizations under both the channels. MBOFDM system with known channel information and perfect synchronization is considered. Relevant parameters are chosen from respective tables .

TABLE 5

ERROR WEIGHTS OF HAMMING		DISTANT FOR RAYLEIGH FADING	
Hamming Distance	Error weights $C_{\tilde{d}}$	Hamming Distance	Error weights $C_{\tilde{d}}$
1	36	11	502960
2	0	12	0
3	221	13	3322763
4	0	14	0
5	1404	15	21292910
6	0	16	0
7	11633	17	134356911
8	0	18	0
9	77433	19	843425871
10	0	20	0



## REFERENCES

- [1] Anuj Batra et al., Texas Instruments et al., "Multi-band OFDM Physical Layer Proposal for IEEE 802.15 Task Group 3a", November, 2003 IEEE P802.15-03/268r2
- [2] Anuj Batra et al. "Design of multiband OFDM system for realistic UWB Channel Environments". IEEE Transaction on Microwave Theory and Techniques, vol. 52, pp. 2123-2138, September 2004
- [3] Sandro Noto, "A MB-OFDM system implemented in Matlab" Project: UWB Receiver: baseband processing using reconfigurable hardware (UWBR) PTDC/EEA-ELC/67993/2006
- [4] M. K. Simon, M-S. Alouini, "Digital Communication over Fading Channel," John Wiley, NJ, USA, 2005
- [5] Herbert E. Saizer, Ruth Zucker, and Ruth Capuano, "Table of the Zeros and Weight Factors of the First Twenty Hermite Polynomials" Journal of Research of the National Bureau of Standards Vol. 48, No. 2, February 1952 Research Paper 2294 pp 111-116
- [6] Debarati Sen, Saswat Chakrabarti, R.V.Raja Kumar, "Some interesting results on compatible BER analysis issues related to multi-band timing and frequency synchronizers applicable for MB-OFDM based UWB communications", Digital Signal Processing 21 (2011) 332-340 @ 2010 Elsevier
- [7] M.-G. Di Benedetto, G. Gianloca, "Understanding ultra wideband radio fundamentals", Pearson Education LPE 2008 ISBN 978-81-317-2279-4
- [8] Jeff Foerster, "Channel Modeling Sub-committee Report" Final IEEE P802.15 Working Group February 2003
- [9] Pal Frenger, Pal Orten, and Tony Ottosson, "Convolutional Codes with Optimum Distance Spectrum" IEEE COMMUNICATIONS LETTERS, Vol. 3, No. 11, November 1999 pp.317-319
- [10] Wang Yanfen Zhang Chuanxiang, "Multipath Channel Model in Underground Mining UWB LOS Environments," IEEE Conference 978-1-4244-3693-4/09/©2009
- [11] Abdellah Chehri, Paul Fortier, Pierre-Martin Tardif, "Frequency domain analysis of UWB channel propagation in underground mines" IEEE Conference -1-4244-0063-5/06 ©2006
- [12] Abdellah Chehri, Paul Fortier, Pierre-Martin Tardif "Measurements and modeling of Line-of-Sight UWB channel in underground mines" IEEE GLOBECOM 2006 proceedings
- [13] SUN Yanjing, PENG Li, LIU Xue, "Wireless Channel Model of UWB for Underground Tunnels in Coal Mine" ©IEEE Conference 978-1-4244-3693-4/09 2009
- [14] Yanjing Sun, Beibei Zhang, "System Model of Underground UWB Based on MB-OFDM" Int. J. Communications, Network and System Sciences, 2011, 4, pp.59-64
- [15] Athar Ravish Khan, Sanjay M. Gulhane, "Performance Evaluation of Time Hopping UWB System in Underground Mine Channel" International Journal of Electronics and Communication Engineering. ISSN 0974-2166 Volume 4, Number 5 (2011), pp. 543-553
- [16] Athar Ravish Khan, Sanjay M.Gulhane, Padmini G. Kaushik "Performance comparison of Ultra Wide Band IEEE Channel and Underground Mine Channel" International Conference on Wireless Communications, Networking and Mobile Computing(WiCom12) Shanghai China . 978-1-61284-683-5/12/ ©2012 IEEE
- [17] Debarati Sen, Saswat Chakrabarti, R. V. Raja Kumar, "Mathematical Analysis of Signal Propagation in Ultra-Wideband Transceiver System with Frequency Offset Correction", 978-1-4244-2644-7/08 © 2008 IEEE
- [18] Debarati Sen, Saswat Chakrabarti, and R. V. Raja Kumar, "Combined BER Analysis for Time-Frequency Synchronization Schemes for MB-OFDM UWB", 978-1-4244-8329-7/11/ ©2011 IEEE
- [19] Standard ECMA-368, "High Rate Ultra Wideband PHY and MAC Standard," 3rd Edition - Dec. 2008, Available at: <http://www.ecmainternational.org/publications/standards/Ecma-368.htm>.
- [20] A Saleh, R Valenzuela., "A Statistical Model for Indoor Multipath Propagation," IEEE JSAC, 1987, vol.5, pp. 128-137.

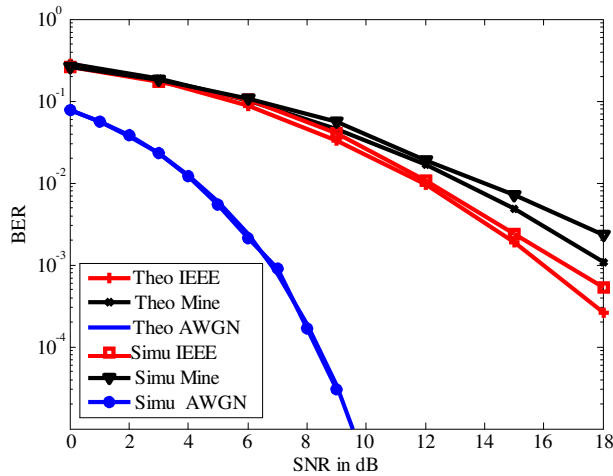


Figure 8: BER of Uncoded MBOFDM system

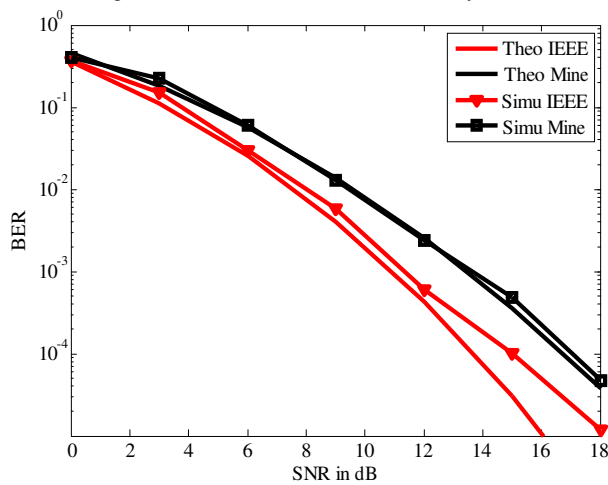


Figure.9 BER of Coded MBOFDM system

## CONCLUSION

we derive the closed form expression of BER of uncoded and convolution coded MB-OFDM UWB system in terms of power decay coefficient for clusters, power decay coefficient for pulse with in clusters, cluster average arrival rate, and pulse average arrival rate with in clusters of UWB channel using Gauss-Hermite quadrature integration. Theoretical and simulation analysis of MBOFDM have been performed for IEEE UWB channel and underground mine channel model. It is observe that the simulation results are nearly close to analytical results which validate the analysis. MBOFDM system is also simulated in AWGN channel and found that simulated values are exactly overlay on theoretical values. A slight deviation in theoretical and simulated BER with increase in SNR is observed and performance difference of about 2dB is observed in underground mine channel as compare to IEEE UWB channel.